Quantum phase transitions in a chain with two- and four-spin interactions in a transverse field

O. F. de Alcantara Bonfim*
Department of Physics, University of Portland, Portland, Oregon 97203, USA

A. Saguia,† B. Boechat,‡ and J. Florencio§
Departamento de Física, Universidade Federal Fluminense Avenida Litorânea s/n, Niterói, 24210-340, Rio de Janeiro, Brazil

(Received 19 August 2013; revised manuscript received 2 August 2014; published 2 September 2014)

We use entanglement entropy and finite-size scaling methods to investigate the ground-state properties of a spin-1/2 Ising chain with two-spin (J_2) and four-spin (J_4) interactions in a transverse magnetic field (B). We concentrate our study on the unexplored critical region $B = 1$ and obtain the phase diagram of the model in the (J_4−J_2) plane. The phases found include ferromagnetic (F), antiferromagnetic (AF), as well as more complex phases involving spin configurations with multiple periodicity. The system presents both first- and second-order transitions separated by tricritical points. We find an unusual phase boundary on the semi-infinite segment ($J_4 < -1$, $J_2 = 0$) separating the F and AF phases.

DOI: 10.1103/PhysRevE.90.032101 PACS number(s): 05.50.+q, 75.10.Pq, 75.10.Jm

I. INTRODUCTION

Ever since its inception by Wu [1] and by Kadanoff and Wegner [2] in 1971, the transverse Ising model with four-spin interactions has attracted a great deal of interest, mainly due to its critical properties. Soon thereafter, Blinc and Zeks [3] suggested that the four-spin interaction could lead to a first-order transition, like the ferroelectric transition of potassium dihydrogen phosphate (KDP). Since that time, the role of multispin interactions in the critical properties of Ising models has been studied by several theoretical methods, such as mean-field [4–6], renormalization group [7,8], Monte Carlo [9,10], series expansions [7,11], and finite-size scaling [12]. Models with four-spin interactions have been used to explain the thermal properties of ferroelectrics $PbHPO_4$ and $PbDPO_4$ [13], binary alloys [9], ferroelectric thin films [14], and copolymers [15]. Recently, there has been a renewal of interest in multispin interactions due to experiments with optical lattices, which can mimic spin Hamiltonians [16–21].

Ultracold atoms trapped in optical lattices allow us to externally induce and control the strong interactions between spin states of neighboring atoms. This opens the possibility of simulating strongly correlated systems in controlled laboratory conditions. In particular, they are suitable for quantum systems modeled by spin Hamiltonians, therefore allowing experimental analysis of the variety of quantum phase transitions present in these systems. By altering the optical potential landscape, the interaction parameters such as magnitude, sign, and anisotropy of the spin Hamiltonians can be fine-tuned to generate novel phases of matter.

These optical lattices operate essentially as quantum simulators, and may help us to understand some challenging problems in condensed matter. The possibility of studying many-body phenomena in this way has attracted a great deal of interest during the last decade [16–21]. Conversely, this has motivated additional numerical simulations in spin systems with complex interactions. These investigations have revealed a rich variety of ground-state configurations and unusual phase transitions [22–28].

It was shown recently that a class of three-spin Hamiltonians can be effectively realized by a triangular optical lattice populated by two fermionic or bosonic atomic species [21,29]. The peculiar form of this interaction comes from the geometry of the lattice that allows for the tunneling of atoms along two different paths. The same type of Hamiltonian can describe the ground-state properties of two species of atoms in a bosonic state trapped in a triangular-ladder configuration. Under these conditions the system shows phases with multiple periodicity, as well as a gapless commensurate chiral phase between the phases with period 2 and 3. Also present in the model are critical points belonging to the same universality class as the Ising and the three-state Potts models [30].

In the present paper, we report our investigations on a quantum spin-1/2 system containing two- and four-spin interactions. We focus our attention on a region not yet explored that reveals a rich variety of quantum phases. We maintain the transverse field at a fixed value, and vary the exchange couplings J_2 and J_4.

In a previous article, Bonfim and Florencio [12] studied the very same model Hamiltonian for $|J_4| < J_2$, and found two transition lines in the ($J_4 - B$) plane of the phase diagram, one of first order and the other of second order. However, the case $|J_4| > J_2$, was not considered there and is the subject of the present work. We were able to fully characterize the ground-state quantum phases. We also determine the nature of the transition lines and multicritical points.

II. MODEL AND NUMERICAL METHODS

We apply two numerical methods used in both statistical physics and information theory. The first is based on the properties of the von Neumann entanglement entropy (EE), while the other relies on finite-size scaling (FSS) analysis. The EE method has been shown to be very precise at locating quantum critical points of a variety of one-dimensional (1D) quantum systems, as well as in the determination of the central

*bonfim@up.edu
†amen@if.uff.br
‡bmbp@if.uff.br
§jfj@if.uff.br

charge of the underlying conformal field theory [31–33]. It is worth mentioning that the central charge c plays an important role in the discussion of universality class of the system. Each universality class corresponds to a distinct value of c. For example, if the system is in the Ising universality class, then $c = 1/2$. On the other hand, for the free bosons, $c = 1$ and for the three-state Potts model, $c = 4/5$. Thus, c is an indicative quantity of the universality class of the system, which determines the critical properties of model. One of the main advantages of the EE method is that it allows for reliable results, even for small lattice sizes, which translates into low computational costs. The FSS method has been used to determine transition lines, critical exponents associated with correlation lengths, and the global properties of various ground states [34].

Consider the 1D Ising model in a transverse field with the addition of four-spin interactions

$$\mathcal{H} = J_2 \sum_i \sigma_i^z \sigma_{i+1}^z + J_4 \sum_i \sigma_i^z \sigma_{i+1}^z \sigma_{i+2}^z \sigma_{i+3}^z + B \sum_i \sigma_i^x. \tag{1}$$

Here σ_i^α is the α component of the Pauli operator located at site i, J_2 is the nearest-neighbor Ising coupling, J_4 the Ising-like four-spin interaction, and B the strength of the magnetic field along the x direction. We use periodic boundary conditions on a chain of N spins, $\sigma_{i+N}^\alpha = \sigma_i^\alpha$.

In this paper, we consider both positive and negative interactions for J_2 and J_4 to explore their relative role on the formation of the quantum phases of the system. The behavior of the system at and around $J_2 = 0$ for nonzero magnetic field has not been properly investigated in the literature, and is one of the points addressed by this paper.

We take the magnitude of the transverse magnetic field $B = 1$ and study the behavior of the model in the parameter space $(J_4 - J_2)$. For $J_4 = 0$ and $J_2 \neq 0$ the model reduces to the usual 1D transverse Ising model, which is exactly solvable and has second-order critical points at $J_2 = \pm 1$ [35]. For $J_2 = 0$ and $J_4 \neq 0$, the system also has two critical points located at $J_4 = \pm 1$ [36,37]. However, the ground-state properties and the precise nature of the transitions at these points are not yet well understood. One of our aims is to examine this problem and to identify the ground-state properties of the system. We wish to establish the nature of the critical points and lines present in the phase diagram of the system.

The following is a description of the methods we use to tackle the problem. In the EE method we consider a system of N spins in a pure quantum state $|\psi\rangle$. Then divide the system into two subsystems $\mathcal{A}$ and $\mathcal{B}$ of sizes l and $N - l$. The entanglement entropy between the two subsystems is given by

$$S(N,l) = -\mathrm{Tr}(\rho_\mathcal{A} \ln \rho_\mathcal{A}), \tag{2}$$

where $\rho_\mathcal{A} = \mathrm{Tr}_\mathcal{B}\, \rho$ is the reduced density matrix of $\mathcal{A}$ after the operators belonging to $\mathcal{B}$ have been traced out. The quantity $\rho = |\psi\rangle\langle\psi|$ is the density matrix of the pure state. Equation (2) is evaluated numerically using $S(N,l) = -\sum \lambda_i \ln \lambda_i$, where λ_i are the eigenvalues of the reduced density matrix $\rho_\mathcal{A}$.

According to conformal field theory, when the system is at criticality, the entanglement entropy assumes the closed form

$$S(N,l) = \gamma \ln \left[\frac{N}{\pi} \sin\left(\frac{\pi l}{N} \right) \right] + \beta, \tag{3}$$

where β is a nonuniversal constant and γ is a constant related to the central charge c [38–42]. In particular, $\gamma = c/3$ when periodic boundary conditions are adopted.

Suppose now that the Hamiltonian of the system depends on a parameter κ, such that, at a quantum transition, $\kappa = \kappa_c$. For $\kappa \neq \kappa_c$, $S(N,l)$ is independent of l and tends to a value $f(\kappa)$ as $N \to \infty$. The order parameter is the difference of the entanglement entropy ΔS between two subsystems of different sizes l and l', both belonging to a system of size N [31,32]. From Eq. (3), as $N \to \infty$ we have

$$\Delta S = S(N,l) - S(N,l') \neq 0 \tag{4}$$

at the critical point, and $\Delta S = 0$ for any value of $\kappa \neq \kappa_c$. Therefore ΔS can be used as an indicator of phase transitions in the infinite-size limit $N \to \infty$. However, this condition is not fulfilled when the system is finite, where it is expected that $\Delta S \neq 0$ for all values of κ. It reaches its maximum at $\kappa = \kappa_c$. As N increases, the peak around κ_c becomes narrower, so that in the infinite-size limit $\Delta S = 0$, everywhere except at that point. Such is the case in a second-order transition.

On the other hand, in a first-order transition $\Delta S \to 0$ everywhere as $N \to \infty$. Hence at the critical point, ΔS is finite for second-order transitions and zero for first-order transitions. In this way ΔS serves as an indicator for both types of transitions. Therefore, for a finite system, a transition point is found by the value $\kappa = \kappa_c$, which maximizes ΔS. The choice of l and l' must satisfy the condition $1 \ll l, l' \ll N$. In addition, finite-size effects on $S(N,l)$ are minimized if we choose them around the middle of the chain [31]. To fulfill these conditions, we use $l = N/2$ and $l' = N/2 - 2$ when a phase of period 2 is present. In the case where a phase of period 4 is present, we use $l = N/2$ and $l' = N/4$. In both cases, those choices are made in order to keep the translational symmetries of the respective ground-states unaffected.

In Fig. 1 we show the entanglement entropy difference of our model, Eq. (1), for some finite chains, as a function of J_2, when $J_4 = 1.3$ and $B = 1$. The location of the transition is obtained from the position of the maxima of ΔS. As we can see the system presents four critical points: $(J_4, J_2) = (1.3, \pm 1.5)$ and $(1.3, \pm 3.0)$. The nature of these transitions is inferred from the dependence of the height of the peak on the system size. Our numerical results show that the heights of $\Delta S_{\max}$ show a tendency to stabilization, as N increases, at those points. Therefore, we conclude that at those points the transitions are all of second order.

To calculate the central charge and discuss the class of universality of the transition we use Eq. (3). By taking two different subsystems of sizes l and l' and subtracting their entropies one from the other, we obtain

$$c = \frac{3\Delta S}{\ln\left[\sin\left(\frac{\pi l}{N}\right) / \sin\left(\frac{\pi l'}{N}\right) \right]}. \tag{5}$$

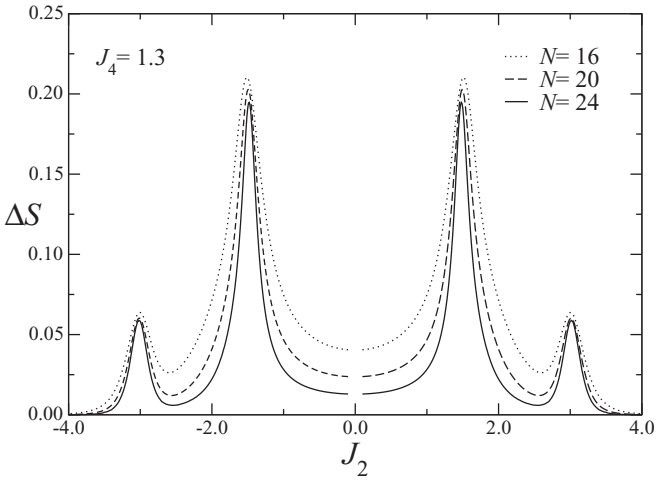

FIG. 1. Entanglement entropy difference $\Delta S = S(N,l) - S(N,l')$ as a function of the coupling J_2, for $J_4 = 1.3$, where $B = 1$ is the energy unit used in all figures in this paper. The positions of the peaks are estimations of four transition points for different values of N, with $l = N/2$ and $l' = N/4$.

If one uses $l = N/2$ and $l' = N/4$, the above equation reduces to

$$c = 6\,\Delta S/\ln(2)\,. \tag{6}$$

By calculating the central charge for several system sizes N, we can estimate its value at the infinite-size limit by extrapolation.

To locate the boundaries between different quantum phases, we also use the FSS method. Suppose now that the Hamiltonian depends on a parameter κ such that at $\kappa = \kappa_c$ the system becomes critical. The energy gap representing the energy difference between the first excited state and the ground state $G(\kappa) = E_1(\kappa) - E_0(\kappa)$ vanishes at the critical point κ_c for an infinite system. For a finite system, the energy gap at the critical point scales with the size of the system N, as

$$G_N(\kappa_c) \equiv \left[E_1^N(\kappa_c) - E_0^N(\kappa_c)\right] \propto N^{-z}, \tag{7}$$

where z is the dynamical critical exponent of the system [43]. However, since the system is conformal invariant $z = 1$. Therefore we shall set the explicit value $z = 1$ in all expressions that follow. The critical parameter $\kappa_c(M,N)$ is estimated by the phenomenological renormalization group relation

$$MG_M(\kappa_c) = NG_N(\kappa_c), \tag{8}$$

where M and N are two distinct lattice sizes.

We employ a modified Lanczos method to calculate the first two lowest energies and their respective eigenstates of the Hamiltonian [44]. Due to computation limitations, the largest size we consider numerically is $N = 24$. To reduce finite-size effects, we find it necessary that N be even for transitions involving antiferromagnetic phases. On the other hand, when a given phase has period 4, N is chosen as a multiple of that peridiocity unit. Those choices preserve the translational symmetry of the ground states. Then the energies are determined as a function of κ. Depending on the size of the system, the ground-state energy is calculated with precision between 10^{-10} and 10^{-12} and the first excited state between 10^{-5} to 10^{-6}. For the location of each point at the critical boundary, we calculate the value of $\kappa = \kappa_c$ at which Eq. (2) is satisfied. This is accomplished by setting $\kappa = J_2$, while keeping J_4 and B as fixed parameters.

To visualize the quantum phases, we consider the relative amplitudes of the basis states forming the ground-state eigenvectors. The spin configuration characterizing each quantum phase is found as follows. The Hamiltonian matrix is written using the standard basis formed by the direct product of the eigenstates $|s\rangle_i$ ($s = 0,1$) of the spin operator $S_i^z, i = 1,\ldots,N$. Thus, we have $|1\rangle_i$ for an up-spin and $|0\rangle_i$ for a down spin at site i. In this notation, an arbitrary basis state for the full Hamiltonian is given by $|n\rangle = \prod_i^N |s\rangle_i$, with the basis state index $n = 0,1,\ldots,P-1$, where $P = 2^N$ is the dimension of the Hilbert space. The basis state index n can be represented by a binary number with N digits. In this notation the value of the bit in the site position i corresponds to the eigenstate of S_i^z. An arbitrary state may be written as a superposition of basis states as follows

$$|\psi_\alpha\rangle = \sum_{n=0}^{P-1} a_\alpha(n)|n\rangle, \tag{9}$$

where α is labels the quantum states. Here, $\alpha = 0$ stands for the ground state and $\alpha = 1$ the first excited state. Because the Hamiltonian matrix is a real and symmetric, the amplitude coefficients $a_\alpha(n)$ are real. As a result the quantum state $|\psi_\alpha\rangle$ can be visualized on a single graph by plotting $a_\alpha(n)$ as a function of the quantum state index n. The graph will completely identify the spatial distribution of spins in the quantum state [12].

III. RESULTS AND DISCUSSION

Our main results are shown in Fig. 2, which depicts the ground-state phase diagram of the model in the $(J_4 - J_2)$ plane. There, we identify antiferromagnetic (AF), ferromagnetic (F),

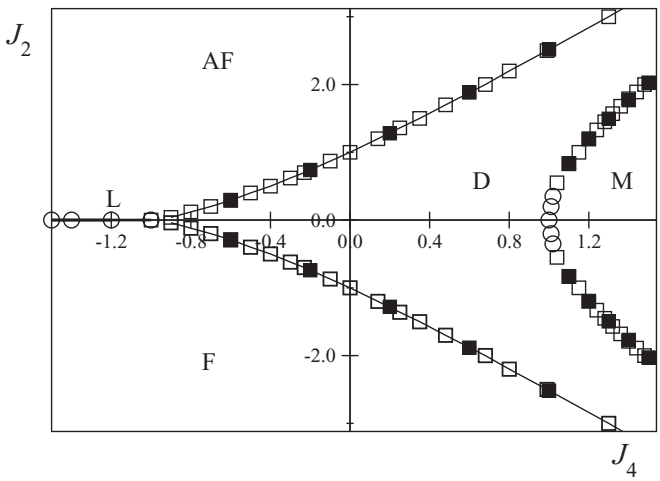

FIG. 2. Phase diagram in the $(J_4 - J_2)$ plane for $B = 1$. Circles and squares indicate first- and second-order transitions, respectively. The phases are as indicated: (F) ferromagnetic; (AF) antiferromagnetic; (D) disordered; and (M) modulated. The nature of each phase is discussed in the text. Open symbols are obtained from entanglement entropy, while solid symbols are from finite-size scaling.

disordered (D), and modulated (M) phases. In the phase boundary (L) between the F and AF phases, there appears an additional ordering, the $\langle 2,2\rangle$ ordering, which is characterized by a sequence of two up-spins followed by two down-spins. The amplitudes corresponding to the $\langle 2,2\rangle$ ordering have negligible contributions in the bulk of the F and AF phases. The phase boundaries are obtained by entanglement entropy (open symbols) and finite scaling methods (solid symbols). Circles and squares identify first- and second-order transition lines, respectively. Thus, the transition lines between the D phase and both the AF and F phases are of second order. The phase diagram Fig. 2 is consistent with the known results, as found in the literature. It reproduces the second-order transition points ($J_4/B = 0, J_2/B = \pm 1$) of the transverse Ising model) [35]. It also agrees with the known results for the system with four-spin interactions in a transverse field ($J_2/B = 0$), in which the phase transitions are located at $J_4/B = \pm 1$ [36,37].

The nature of each phase is characterized by the relative amplitudes of the the basis states in the ground-state wave vector. By identifying the largest amplitudes that makeup the ground-state, one can infer the phase ordering. To illustrate the nature of the phases in the phase diagram, we consider the case of a system of size $N = 8$. Larger system sizes, such as $N = 12, 16, 20$, and 24, show essentially the same features, but the pictures become too dense due the exponential growth of the number or states so that we cannot display them here. As long as the lattice size is a multiple of 4, the phase diagram will be essentially the same as that one shown in Fig. 2. In the AF region of the phase diagram, the states $|85\rangle = |01010101\rangle$ and $|170\rangle = |10101010\rangle$ have noticeable amplitude contributions to the ground state. The amplitudes of all the basis states forming the ground state are shown in Fig. 3, for the case $(J_4, J_2) = (0.5, 2.0)$, which is within the AF phase. On the other hand, all the contributions to the ground state for the case $(J_4, J_2) = (0.5, -2.0)$, inside the F phase, can be visualized in Fig. 4, for $(J_4, J_2) = (0.5, -2.0)$. As can be seen, the basis states $|0\rangle = |00000000\rangle$ and $|255\rangle = |11111111\rangle$ have the largest amplitudes forming the ground state. In each of these figures, there is a background of noise-like amplitudes, which are caused by the transverse magnetic field, a purely quantum effect. Such background amplitudes appear in all phases and, as a rule, the larger the transverse field the greater the amplitudes of the background states.

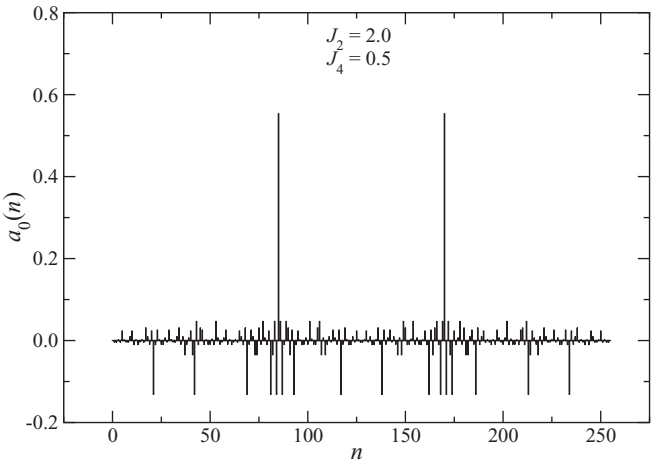

FIG. 3. Ground-state amplitude $a_0(n)$ plotted against the basis state index n for $(J_4, J_2) = (0.5, 2.0)$ and $N = 8$. The two largest amplitudes at $n = 85$ and 170 correspond to antiferromagnetic ordering. The transverse magnetic field induces the smaller amplitudes.

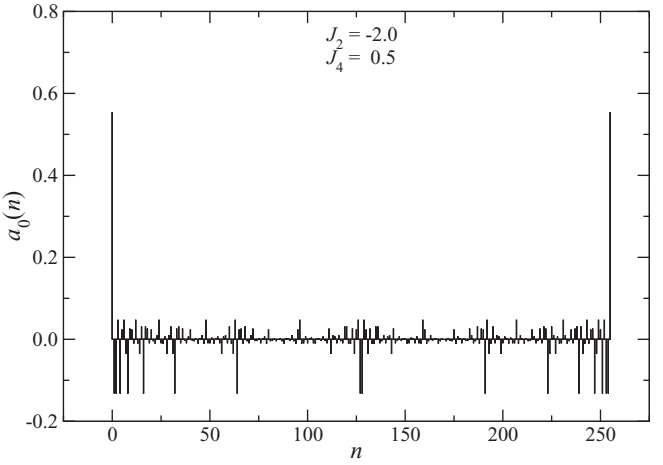

FIG. 4. Ground-state amplitude $a_0(n)$ against the basis state index n for $(J_4, J_2) = (0.5, -2.0)$ and $N = 8$. The two largest amplitudes at $n = 0$ and 255 correspond to ferromagnetic ordering.

Figure 5 shows how the central charge c varies with the system size N along the AF critical line, for $J_4 = 0.3$ and 0.8. We used $l = N/2$ and $l' = N/2 - 2$, so that the central charge is now given by

$$c = -\frac{3\,\Delta S}{\ln[\cos(2\pi/N)]}. \tag{10}$$

The figure indicates that at the infinite-size limit the central charges approach the asymptotic value $c = 0.5$, which is the known value of the central charge for the transverse Ising model. Other values of J_4 yield the same asymptotic value for c. The convergence to the asymptotic value is faster near

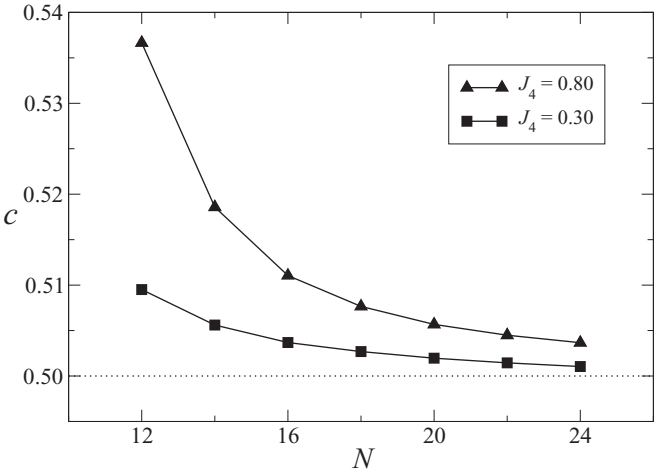

FIG. 5. Dependence of the central charge with system size along the transition line separating the antiferromagnetic and disordered phases, for the case $J_4 = 0.8$ and 0.3, The dotted line indicates the asymptotic value of the central charge at the infinite-size limit.

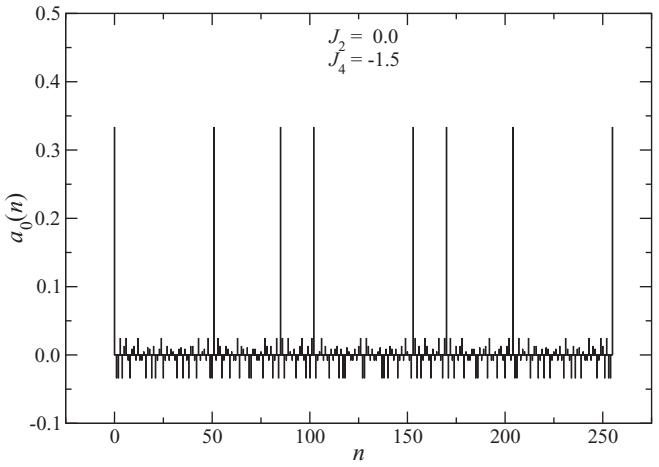

FIG. 6. Ground-state amplitude $a_0(n)$ as a function of the basis state index n for $(J_4, J_2) = (-1.5, 0.0)$ and $N = 8$. It consists of a linear combination of three orderings: ferromagnetic, antiferromagnetic, and $\langle 2,2\rangle$. The smaller amplitudes correspond to low probability configurations induced by the transverse magnetic field.

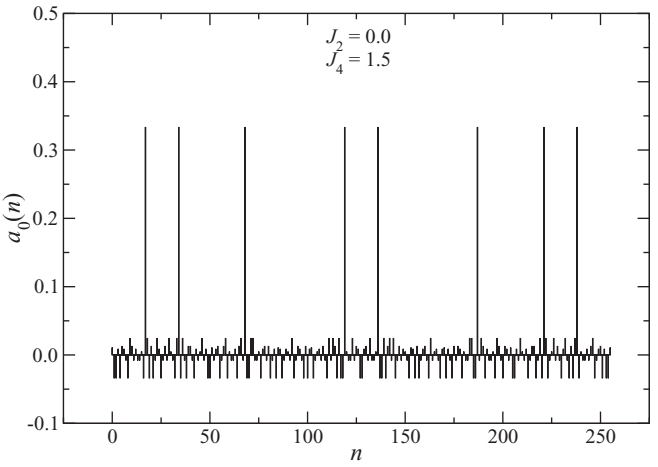

FIG. 8. Ground-state amplitude $a_0(n)$ as a function of the basis state index n for $(J_4, J_2) = (1.5, 0.0)$ and $N = 8$. The predominant state, with largest amplitudes, is the $\langle 3,1\rangle$ with a small disordered background induced by the transverse magnetic field.

the transverse Ising model critical points $(J_4, J_2) = (0.0, 1.0)$. Similar results are found along the ferromagnetic critical line in the lower part of the phase diagram.

The second-order transition lines separating the F and AF phases from the disordered phase merge at $(J_4, J_2) = (-1.0, 0.0)$. Along the boundary line $(J_4 \leqslant -1,\ J_2 = 0)$ the ground state is formed by three coexisting orderings: AF, F, and $\langle 2,2\rangle$. The amplitudes of their basis states occurring in the ground state are shown in Fig. 6, for $(J_4, J_2) = (-1.5, 0.0)$, in a chain of size $N = 8$. There, eight basis vectors have amplitudes that stand out from the noise-like background. We should note that the $\langle 2,2\rangle$ ordering appears only at the phase boundary L. As one moves away from that line, entering the AF (F) region, the only prominent contribution are those of the AF (F) phase.

The entanglement entropy difference ΔS, as a function of the coupling J_2, with $J_4 = -1.3$, is shown in Fig. 7. The figure

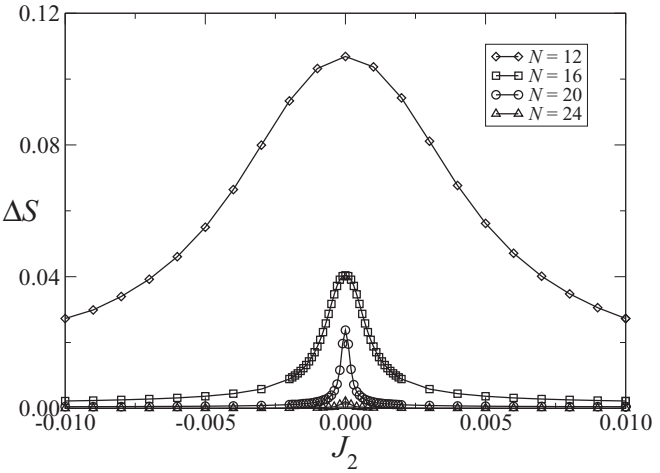

FIG. 7. Entanglement entropy difference ΔS as a function of the two-spin coupling J_2, for $J_4 = -1.3$ and different chain sizes. Notice the reduction of the maximum of ΔS the at $J_2 = 0$ as N increases.

displays results for the system sizes $N = 12, 16, 20$, and 24. As ΔS crosses the the boundary L, there is a noticeable maximum at $J_2 = 0$. However, as N increases, $\Delta S \to 0$, thus indicating that it is a first-order transition line. We find a multicritical point at $(J_4, J_2) = (-1.0, 0.0)$.

The amplitudes of the basis states forming the ground state at $(J_4, J_2) = (1.5, 0.0)$ are shown in Fig. 8. The ground state is predominantly formed by the $\langle 3,1\rangle$ states, together with a background induced by the transverse magnetic field. The $\langle 3,1\rangle$ states consist of sequences of clusters with three up (down) spins followed by one down (up) spin. For $N = 8$, the basis vectors composing the $\langle 3,1\rangle$ ground state are $|17\rangle = |00010001\rangle$, $|34\rangle = |00100010\rangle$, $|68\rangle = |01000100\rangle$, and $|136\rangle = |10001000\rangle$, with net down-magnetization; $|119\rangle = |01110111\rangle$, $|187\rangle = |10111011\rangle$, $|221\rangle = |11011101\rangle$, $|238\rangle = |11101110\rangle$, with net up-magnetization. In the region denoted by M of the phase diagram, the $\langle 3,1\rangle$ states contribute with the largest amplitudes to the ground states. Hence we call that region the modulated phase M.

Figure 9 shows the maximum of the entanglement entropy difference $\Delta S_{\max}$ versus the system size N for several values of the two-spin coupling J_2, along the critical line. As we pointed out earlier, we can use only lattice sizes which are multiples of 4, which is the periodicity of the modulated phases $\langle 3,1\rangle$ involved in the transitions. Nonetheless, we still can make claims about the nature of the transitions based on the entropy of entanglement method. We note that for larger values of J_2, $\Delta S_{\max} \to 0$ as N increases, thus indicating transitions of first-order. For small J_2, $\Delta S_{\max}$ rises to a nonzero value, a signal of second-order transitions. The boundaries of the modulated $\langle 3,1\rangle$ phase shown in Fig. 2 are of either first- or second-order transitions. The lines join at the two tricritical points, located at $(J_4, J_2) = (1.04 \pm 0.01, \pm 0.55 \pm 0.01)$. For $|J_2| < 0.55$, the line corresponds to first-order transitions (circles). Otherwise, they are second-order transition lines (squares). In particular, at $(J_4, J_2) = (1.0, 0.0)$, the transition is of first order. This

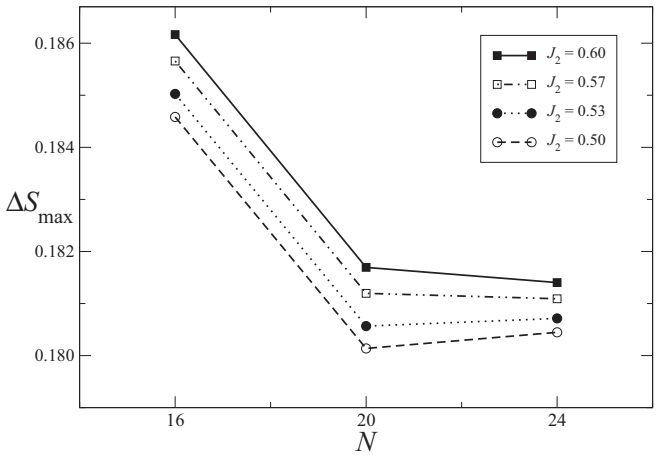

FIG. 9. Maximum of the entanglement entropy difference ΔS_{max} against N for several values of the two-spin coupling J_2 on the transition line. The tricritical point is located at $J_2 = 0.55 \pm 0.01$, where there is a noticeable change in the direction of ΔS_{max} as N increases.

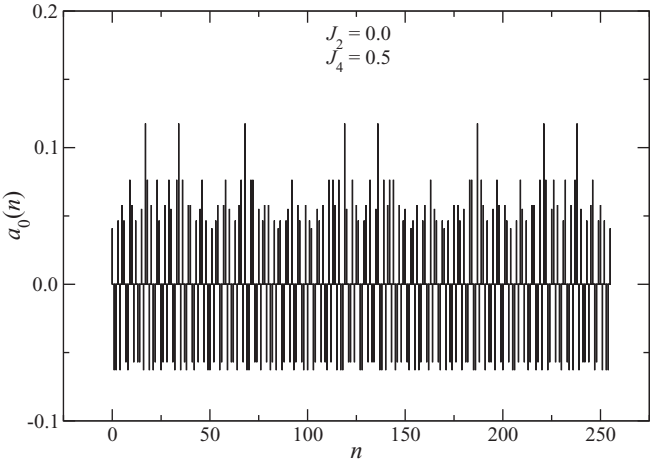

FIG. 10. Ground-state amplitude $a_0(n)$ as a function of the basis state index n for $(J_4, J_2) = (0.5, 0.0)$ and $N = 8$. Here the ground state is in the disordered phase.

confirms a conjecture found in the literature that the transition might be of first order [45].

The disordered phase D, in the middle region of the phase diagram, has basis state amplitudes of about the same strength, as shown in Fig. 10. Notice, though, that the $\langle 3,1 \rangle$ basis states contribute with amplitudes slightly larger than those of the remaining basis states. For points farther away from the boundary lines, contributions from ordered states become less relevant.

IV. CONCLUDING REMARKS

To summarize, we investigated the ground-state phase diagram of the transverse Ising model with additional four-spin interactions, using finite-size scaling and entanglement entropy methods. In our work, we considered the quantum system with $B = 1$, and unraveled a rich phase diagram with both conventional F and AF orderings, as well as more complex spin orderings, such as $\langle 3,1 \rangle$ and $\langle 2,2 \rangle$. The phase diagram contains tricritical points, a multicritical point, and an interesting phase boundary between the AF and F phases. The model studied here could possibly be realized in optical lattices, just like the case of the transverse Ising model recently reported [16].

ACKNOWLEDGMENTS

We thank FAPERJ, CNPQ, and PROPPI/UFF (Brazilian agencies) for financial support. O.F.A.B. acknowledges support from the Murdoch College of Science Research Program and a grant from the Research Corporation through the Cottrell College Science Award No. CC5737.

[1] F. W. Wu, Phys. Rev. B **4**, 2312 (1971).
[2] L. P. Kadanoff and F. J. Wegner, Phys. Rev. B **4**, 3989 (1971).
[3] R. Blinc and B. Zeks, Adv. Phys. **21**, 693 (1972).
[4] C. L. Wang, Z. K. Qin, and D. L. Lin, J. Magn. Magn. Mater. **88**, 87 (1990).
[5] K. G. Chakraborty, J. Magn. Magn. Mater. **114**, 155 (1992).
[6] T. Kaneyoshi and T. Ayoama, J. Magn. Magn. Mater. **96**, 67 (1991); B. Laaboudi and M. Kerouad, *ibid.* **164**, 128 (1996).
[7] M. P. Nightingale, Phys. Lett. A **59**, 486 (1977).
[8] J. M. J. van Leeuwen, Phys. Rev. Lett. **34**, 1056 (1975); F. Lee, H. H. Chen, and F. Y. Wu, Phys. Rev. B **40**, 4871 (1989).
[9] D. F. Styer, M. K. Phani, and J. L. Lebowitz, Phys. Rev. B **34**, 3361 (1986).
[10] K. K. Chin and D. P. Landau, Phys. Rev. B **36**, 275 (1987); G. M. Zhang and C. Z. Yang, *ibid.* **48**, 9487 (1993); J. R. Heringa, H. W. J. Blöte, and A. Hoogland, Phys. Rev. Lett. **63**, 1546 (1989).
[11] D. W. Wood and H. P. Griffiths, J. Phys. C **7**, L54 (1974); H. P. Griffiths and D. W. Wood, *ibid.* **7**, 4021 (1974).
[12] O. F. de Alcantara Bonfim and J. Florencio, Phys. Rev. B **74**, 134413 (2006).
[13] W. Chunle, Q. Zikai, and Z. Jinghbo, Ferroelectrics **77**, 21 (1988).
[14] B. H. Teng and H. K. Sy, Europhys. Lett. **73**, 601 (2006).
[15] P. R. Silva, B. V. Costa, and R. L. Moreira, Polymer **34**, 3107 (1993).
[16] J. Simon, W. S. Bakr, R. Ma, M. E. Tai, P. M. Preiss, and M. Greiner, Nature (London) **472**, 307 (2011).
[17] D. Jaksch, C. Bruder, J. I. Cirac, C. W. Gardiner, and P. Zoller, Phys. Rev. Lett. **81**, 3108 (1998).
[18] A. Kastberg, W. D. Phillips, S. L. Rolston, R. J. C. Spreeuw, and P. S. Jessen, Phys. Rev. Lett. **74**, 1542 (1995); G. Raithel, W. D. Phillips, and S. L. Rolston, *ibid.* **81**, 3615 (1998).
[19] M. Greiner, O. Mandel, T. Esslinger, T. W. Haensch, and I. Bloch, Nature (London) **415**, 39 (2002); M. Greiner, O. Mandel, T. W. Haensch, and I. Bloch, *ibid.* **419**, 51 (2002).

[20] O. Mandel, M. Greiner, A. Widera, T. Rom, T. W. Haensch, and I. Bloch, Nature (London) **425**, 937 (2003).
[21] J. K. Pachos and E. Rico, Phys. Rev. A **70**, 053620 (2004).
[22] A. Kuklov, N. Prokof'ev, and B. Svistunov, Phys. Rev. Lett. **92**, 050402 (2004).
[23] B. Paredes, A. Widera, V. Murg, O. Mandel, S. Fölling, I. Cirac, G. V. Shlyapnikov, T. W. Haensch, and I. Bloch, Nature (London) **429**, 277 (2004).
[24] A. B. Kuklov and B. V. Svistunov, Phys. Rev. Lett. **90**, 100401 (2003).
[25] D. Jaksch and P. Zoller, New J. Phys. **5**, 56 (2003).
[26] L. M. Duan, E. Demler, and M. D. Lukin, Phys. Rev. Lett. **91**, 090402 (2003).
[27] P. Fendley, K. Sengupta, and S. Sachdev, Phys. Rev. B **69**, 075106 (2004).
[28] C. M. Dawson and M. A. Nielsen, Phys. Rev. A **69**, 052316 (2004).
[29] J. K. Pachos and M. B. Plenio, Phys. Rev. Lett. **93**, 056402 (2004).
[30] C. D'Cruz and J. K. Pachos, Phys. Rev. A **72**, 043608 (2005).
[31] J. C. Xavier and F. C. Alcaraz, Phys. Rev. B **84**, 094410 (2011).
[32] S. Nishimoto, Phys. Rev. B **84**, 195108 (2011).
[33] A. Saguia, Phys. Lett. A **377**, 2288 (2013).
[34] P. R. C. Guimarães, J. A. Plascak, F. C. Sá Barreto, and J. Florencio, Phys. Rev. B **66**, 064413 (2002).
[35] P. Pfeuty, Ann. Phys. (NY) **57**, 79 (1970).
[36] L. Turban, J. Phys. C **15**, L65 (1982).
[37] K. A. Penson, R. Jullien, and P. Pfeuty, Phys. Rev. B **26**, 6334 (1982).
[38] G. Vidal, J. I. Latorre, E. Rico, and A. Kitaev, Phys. Rev. Lett. **90**, 227902 (2003).
[39] P. Calabrese and J. Cardy, J. Stat. Mech. (2004) P06002.
[40] C. Holzhey, F. Larsen, and F. Wilczek, Nucl. Phys. B **424**, 443 (1994).
[41] P. Calabrese and J. Cardy, J. Phys. A: Math. Theor. **42**, 504005 (2009).
[42] I. Affleck and A. W. W. Ludwig, Phys. Rev. Lett. **67**, 161 (1991).
[43] M. Barber, *Phase Transition and Critical Phenomena*, Vol. 8, (Academic Press, New York, 1993).
[44] E. Dagotto and A. Moreo, Phys. Rev. D **31**, 865 (1985); E. R. Gagliano, E. Dagotto, A. Moreo, and F. C. Alcaraz, Phys. Rev. B **34**, 1677 (1986).
[45] K. A. Penson, Phys. Rev. B **29**, 2404 (1984).